UNIVERSITÀ DEGLI STUDI DI PADOVA

DIPARTIMENTO DI INGEGNERIA DELL'INFORMAZIONE

DIPARTIMENTO DI INGEGNERIA DELL'INFORMAZIONE

CORSO DI LAUREA MAGISTRALE IN BIOINGEGNERIA

Influence of tractogram filtering in analysis of tractography data in rat brains

Relatore:

Prof.ssa Alessandra Bertoldo

Supervisore:

Prof. Rodrigo Moreno

KTH Royal Istitute of Technology

Candidato:

Filippo Maschio

ANNO ACCADEMICO 2021/2022

15 Dicembre 2022

Abstract

Neuronal disorders could result in changes at brain connectomics level. One of the main goal of structural connectomics analysis deals with the possibility to detect the changes at neuronal level by studying brain connectivity. These result is possible by generating the tractography maps from diffusion MRI data, however, the algorithms for this step are affected by high sensitivity and low specificity. As a consequence, this technique could lead to result not completely reliable, with many false positive. New techniques based on tractograms filtering have been developed to resolve the problem.

This thesis studies the impact of tractogram filtering for rats brain diffusion data (divided in rats with and without hearing problems) analyzing the changes on structural connectivity derived from tractograms considering the hearing cortex areas. In particular, Spherical-deconvolution informed filtering of tractograms (SIFT) has been used as filter. Furthermore, after the analysis of structural connectivity, a statistical based approach has been uses to classify the connectivity matrices to analyse if there was any difference between unfiltered and filtered data performance.

Metrics extracted from the connectivity matrices showed differences between the unfiltered and filtered data considering the single nodes. This means the connectomes changed and, in particular, the main connections. Connectomes weighted by Fractional Anisotropy (FA), Mean Diffusivity (MD) and Radial Diffusivity (RD) showed similar results. Statistical analysis based on classification performed better in average with filtered matrices as input. The biggest difference has been observed with raw data, 27.27% more accurate for filtered data.

These are the limitations of the study: number of subjects was small, Region of Interest (ROI) masks were hand made (not default atlas) and needed manual registration.

Acknowledgments

There are many people I want to thank for helping and supporting me through the my personal life and the development of this thesis during this past year. First of all I want to thank my family, composed by my mother, my father and my brother, for all the support and belief in myself, it would have been much harder without them. Secondly, I want to thank my international supervisor during the Erasmus exchange, Rodrigo Moreno, for being a reference to me during this long project and for letting me be part of his group at KTH university. A big thank you to my roommate and all my office mates, we shared a lot of opinions and fun times working at our thesis. Finally, I want to say thank you to all the people, both international and not, that have been a part of my last year. In particular I want to cite my closer friends, my girlfriend and all the amazing people I spent most time during my exchange period, they will be forever part of my soul. It has been the most amazing year of my life, both for my professional and personal life, and it would not have been the same without all these people I cited.

"Per aspera ad astra"

Contents

Abbreviations

SIFT Spherical-deconvolution informed filtering of tractograms

FA Fractional Anisotropy

MD Mean Diffusivity

RD Radial Diffusivity

ROI Region of Interest

AC Auditory Cortex

CN Cochlear Nuclear Complex

IC Inferior Collicus

MG Medial Geniculate Body

SOC Superios Olivary Complex

FOD Fiber orientation distribution

WM white matter

GM grey matter

CSF Cerebrospinal fluid

CTRL *control*

OBST *patient*

MRI Magnetic Resonance Imaging

1 Introduction

Analysis of lab animals brain (like rats, mice and rodents) permit to have a preliminary study and result of the human brain. This is possible due to the very similar cerebral structure organizations that allows to have an idea of what to expect from human brain analysis before doing them [27].

It is possible to better understand brain disease by studying brain connectivity. Auditory system is just one example of brain cortex that is formed by multiple regions (rats' anatomy at section 6.6) that communicate each to work. However, these connection could be altered by a brain disease.

Starting from image technique diffusion magnetic resonance imaging (dMRI) is possible to extract the the fiber pathways in the brain. This evaluation is possible thanks to the motion of water molecules along the neuronal axons (section 6.1). Considering specific predefined areas is possible to extract the connectivity between these areas, characterized by the tracts that connect them. However, the traditional techniques to perform tractography suffer of high sensitivity and low specificity. This problem could lead to have a lot of false positive (section 6.2) so the need to discover and use new techniques is evident. To resolve this problem, it has been developed a technique based on filtering the tracts from the traditional tractography (section 6.4). There are many possible way to perform it and the firsts studies are promising [26].

The aim of this study is to verify if tractogram filtering influence and improves the traditional tractography. This analysis is performed with statistical analysis of connectoms (unfiltered and filtered) extracted from a group of rat brains divided by *control* subjects without any disease and *patient* subjects affected by hearing problems. The analysis is focused on the hearing cortex.

2 Methods

In this chapter all the methodologies to process the data are presented. Starting from the data-set (section 2.1) composed by diffusion and structural data of 11 different rats, divided in *patient* (OBST) and *control* (CTRL) subjects, the data were processed to be prepared for extraction of tractography (section 2.2.1) and the application of tractogram filtering (section 2.2.2). Then a parcellation map was built from ROIs masks (section 2.3.1) to evaluate the connectivity matrices (section 2.3.2). The final step has been the extraction of different metrics from the connectivity matrices (section 2.4) and to perform statistical analysis (section 2.5) between the two groups of subjects (OBST and CTRL) to evaluate the differences.

2.1 Data

The rats ex-vivo were perfused with intravenous normal saline, and then fixated with intravenous formaldehyde. The brains were put in fomblin solution before scanning. The data extraction took several hours to be completed.

The dataset is composed by a subest of diffusion magnetic resonance images dMRI) and a set of 10 different ROI masks of the cortex related to auditory nerve system for each subject. Here are the 10 regions (for both brain hemispheres): Auditory Cortex (AC), Cochlear Nuclear Complex (CN), Inferior Collicus (IC), Medial Geniculate Body (MG) and Superios Olivary Complex (SOC). The dataset and the masks were preprocessed by Karolinska Institutet of Stockholm. The images are from 11 different rats ex-vivo (12 months old), 7 of them were diagnosed with auditory problems and belong to the OBST class, meanwhile the other 4 had not any auditory problem and belong to the CTRL class. The diffusion images contain 48 axial slices with 48 diffusion-weighted directions (b= 1250 s/mm^2), the voxels size is 0.1125x0.15x0.15 mm^3. The masks have been created manually by a doctor at Karolinska institutet.

2.2 Region of Interest Masks Processing

Some discrepancies between the orientation of the masks and the diffusion images, they were not overlaying correctly. In fact the ROI masks were originally created for the same dMRI images but before the processing, therefore the b-value of the dataset held was not correct for these images were the masks were fitting. This problem has been faced trying to use many tools for images registration. The final decision was to impose to the masks images the same q-form of the diffusion images and to manually rotate the masks around one of the axis. The q-form was imposed through the function *fslorient* of the software *FSL* (https://fsl.fmrib.ox.ac.uk/fsl/fslwiki). For the manual registration has been used an image processing module from software MeVisLab (https://www.mevislab.de/). For each mask it has been tried to reach the best result in matching the right brain area.

The registration was a necessary step due to use the masks to analyze the ROIs in the tractograms and in the connectivity matrices and to build a parcellation map (needed for connectivity matrix evaluation).

2.3 Tractography

Tractography is a technique used to reconstruct brain neural fiber pathway. It can be computed using different type of approach, the principal one are probabilistic and deterministic. In this case the tractograms have been evaluated through the iFOD2 algorithm (probabilistic approach). The iFOD2 algorithm is better for crossing fiber reconstruction [32] . However, this neuronal fiber reconstruction suffer from low specificity. For this reasons, tractogram filtering algorithm technique SIFT [22] is applied to the tractograms evaluated by the algorithm iFOD2. Both SIFT and iFOD2 were applied to the data through the software *MRtrix3* (https://www.mrtrix.org/).

2.3.1 Tractogram Generation

To compute the tractograms from the data it as been used *MRtrix3* software, as said in the previous section. In particular, it has been chosen the *tckgen* script, that requires some specific prerequisites starting from the generation of the Fiber orientation distribution (FOD). The FODs were computed through the *MRtrix* script *dwi2fod* using the *csd* algorithm, that is designed for single-shell data and only uses a single b-value. Moreover, the response functions for white matter (WM), grey matter (GM) and Cerebrospinal fluid (CSF) is required for FODs extraction. therefore, response functions were evaluated for each subject with *dwi2response* script and the *dhollander* algorithm.

To run the final script is necessary to choose the algorithm to use (iFOD2 in this case), a tractography seeding mechanism. For the seeds it has been used a mask created from the ROIs, specific for each subject, where the streamlines were imposed to start. Moreover, it has been imposed other parameters: first of all a mask corresponding to the whole brain for the streamlines were allowed to go. Afterwards, it has been decided for the number of streamlines to find, the minimum length and the cutoff as shown in table 1. These parameters have been changed from the one used in other papers [26, 38] for similar goals. The reason of these choices has been the good results obtained by the other papers and have been adjusted to this case. The idea was to start with a lower number of streamlines and to grow it, while changing *minlenght* and *cutoff* values. The initial number for streamlines was one million but the results were not promising. Looking at the results visually it was possible to valuate the parameters if they were good enough or not.

Table 1: parameters used to compute all the tractograms with *tckgen* script. *-select* is the number of streamlines to find, *-minlength* is the minimum length for the streamlines in *mm*, *-cutoff* set the FODs amplitude. Other parameters were *-mask* and *-seed_image*

Parameters		
-select	*-minlength*	*-cutoff*
7000000	2	0.08

2.3.2 Tractogram Filtering

The filtered tractograms were generated using the algorithm SIFT through the *MRtrix3* script *tcksift*. To make it run is necessary to give as input the tractograms evaluated and the FODs response for the WM. It has been imposed a threshold to stop the extraction of the filtered tractograms after a certain input: 700'000 tracts. The ratio between the starting number of streamlines and the number of streamlines to leave after filter application is 1/10 according to a similar study applied to human brain [26]. The other option was to use SIFT2 algorithm but it uses a different approach. In fact, it assign a weight to each streamlines without deleting them [22]. Since the data are not human, it would have been difficult to regulate this algorithm and choose the right threshold.

2.4 Connectivity Matrix

The connectivity matrices were extracted both for raw tractograms and filtered tractograms taking in account only the ROIs of the dataset, the software used was *MRtrix3*. In order to evaluate the matrix, it has been necessary to create a parcellation map starting from the 10 masks. Afterwards, the space dimension for the matrices was 10x10, each element of the matrix correspond to the edge between two regions. From this matrices it was possible to start the analysis on metrics obtainable.

To have different points of view, the matrices and the metrics were evaluated

considering 4 different weights for the connections: no weights, FA weighted, MD weighted and RD weighted. For each weight have been created 22 matrices, for each subject 8 matrices.

2.4.1 Connectivity Matrices Generation

The script used to evaluate the connectivity matrices was *tck2connectome* (provided by *MRtrix3*). In the case on no weights on the connections, the inputs required are the streamlines file (filtered or not) and the node parcellation file, the output is the metric of connectitvity quantified in the matrix as the number of streamlines. The parcellation map has been created assigning a unique number to each of the 10 ROIs mask and putting them in a single NifTI file.

To create weighted matrices it has been used one of the option of the same script, *tck2connectome*, that allows to scale each stramlines by weight individually in another file. In order to do that, it was necessary to extract the weighted images from the diffusion data using the estimation of the diffusion tensor, evaluated through the *dwi2tensor* script from *MRtrix3*, and than by using the *tensore2metric* script with the chosen option for the chosen image (*-fa*, *-rd* or *-adc*, corresponding to FA, RD and MD). Both these script were provided by *MRtrix3*. To scale the streamlines it has been used the script *tckscale* (by *MRtrix3*) giving as input the the streamlines file, the weighted image (FA, MD or RD) and using the option *-stat_tck* to get the mean. For each streamline, the value of the underlying weighted image is sampled for each vertex and the mean is calculated to have a single value for streamline. Then the contribution of each streamline that was assigned to the nodes of connectome is multiplided with the mean calculated prior for that specific streamline. Finally, for each connectome edge, a mean of the values assigned by all the streamlines mean is calculated. Afterwards, the oputput of *tcksample* has been given to *tck2connectome* with the option *-scale_file*. Even in this case, to have a single value, it has been imposed to get the mean with the option *-stat_edge*.

The generated matrices were imposed to be symmetric with the parameter

-symmetric. Additionally, the self-connection of each region (diagonal values of the matrix) has been imposed equal to zero with parameter *-zero_diagonal*.

2.4.2 Connectivity Metrics

From the connectivity matrices have been extracted some connectivity metrics to evaluate a difference between the filtered matrices and the unfiltered matrices. All the metrics operation have been implemented through the python library *networkX* (https://networkx.org/).

The first metric evaluated was the *betweenness centrality* (1) for each node (v) and for each graph (weighted and not), that is the is the sum of the fraction of all-pairs shortest paths that pass through that specific node.

$$c_B = \sum_{s,t \in V} \frac{\sigma(s,t|v)}{\sigma(s,t)} \tag{1}$$

Where V is the set of nodes, $\sigma(s,t)$ is the number of shortest (s,t)-paths, and $\sigma(s,t|v)$ is the number of those paths passing through some node v other than s,t. Secondly, it has been evaluated the *eigenvector centrality* (2) for each matrix, it computes the centrality for a node based on the centrality of its neighbors. The eigenvector centrality for node i is:

$$Ax = \lambda x \tag{2}$$

Where A is the adjacency matrix of the graph, with eigenvalue λ. Thirdly, it has been extracted the *node strength* (3) from each node of the different matrices. It is the reflex of the property of a node to connect to others with a high number of connections or weights. The *node strength* is calculated for node i with the formula:

$$S_i = \sum_{j=1}^{n} A_{ij} \tag{3}$$

S is a one dimensional vector with n elements (n is the number of nodes). The last metric considered has been the *global efficiency* for each subject. The

efficiency of a pair of nodes in a graph is the multiplicative inverse of the shortest path distance between the nodes. The average global efficiency of a graph is the average efficiency of all pairs of nodes.

The goal of the evaluation of the metrics is to make a comparison of the output values through the subjects between the matrices filtered and unfiltered. It has been taken in account some of the most used metrics to describe graghs and their characteristics.

2.5 Statistical Analysis

Statistical analysis has been evaluated to compare the performances of some statistical techniques on two different input, filtered and unfiltered. The idea is to extract the accuracy on predicting the class of *CTRL* rats and *OBST* rats, and to compare the result for the same datasets before and after the filter SIFT application. The environment used to perform the statistical computation and graphics is R software (https://www.r-project.org/).

2.5.1 Datasets Creation

A fundamental step of the analysis was the creation of the datasets. The final choice was between datasets with the following two structures: the first structure was thought as a dataset with 11 rows (one for each rats), or observations, and 52 columns, or features. The columns were decided to represent one of the connectivity metrics evaluated for each of the node. Moreover, the same dataset, would have included the metrics of the nodes for the weighted matrices too (FA, MD and MD). Therefor, the output would have been two datasets 11x52 for the unfiltered and filtered data. The second structure considered presents 11 rows, as the other propose, and 55 columns. Each of the columns represents the connectivity between two nodes. therefor, in this case were considered directly the matrices as input, and not the metrics extracted. Another different is the number of datasets, in fact, this second propose, has a total of 8 datasets, 4 for the unfiltered matrices and 4 for the filtered matrices (raw, FA, MD and MD).

For both the proposes, there was an additional column called "class" to set the category of each of the 11 rats (*OBST* or *CTRL*).

Both datasets were tried and the second structure has been chosen for the final statistical analysis. This decision was due to the possibility to divide the analysis for each weight of the matrices.

2.5.2 Classification Methods

The analysis is based on a binary classification based on the feature *class*, described in the previous sub-paragraph. The techniques chosen for this goal are the supervised learning methods *Random Forest* and *Naive-Bayes*. Both these algorithms are applicable when there are more features than observations, and both binary and multi-category classification tasks. Moreover, Naive-Bayes, permits to value and visualize the influence of each feature based on the distribution of the features for the two classes. Random Forest, instead, performs embedded features selection, important for the next analysis step, incorporates interactions between features [34, 35].

Other binary classification techniques have been considered as logistic regression, but it seemed to be a too simplistic model with these particular datasets. Support vector machines was discarded for the high number of parameters to set, not easy to balance. K-Nearest neighbours was avoided due to the small number of observation.

To train the model of random forest and Naive-Bayes it has been used a leave one out cross validation considering there are just 11 observations. Moreover, the metric considered as output is accuracy. The reliability of the results has been evaluated through the Kappa statistic. It is relevant to know that for Random Forest and Naive-Bayes there are some parameters as output that define the best model (the parameters name are typical of the software R managing with Random Forest and Naive-Bayes specifically). For Rondom Forest is the number of features, called *mtry*, used to split the trees. Instead, for Naive-Bayes, there is the parameter kernel with output *true* or *false*. If *true*, a kernel density

estimation (KDE) can be alternatively used to obtain a non-parametric representation of the conditional probability density function instead of the Gaussian distribution (*false*).

2.5.3 Features Analysis

After the classification step, the most relevant features have been extracted from each datasets to compare the outputs between the unfiltered and the filtered one. In order to do this has been used an algorithm based on random forest called *Boruta* (https://www.rdocumentation.org/packages/Boruta), from software R. This package is able to classify the features of a datasets as important or not important by training the dataset and considering the mean decrease accuracy of each features (in this case has been used 1000 iteration, the maximal number of importance source runs, to resolve the most of the attributes left as tentative). The goal is to discuss the differences and to perform again the classification with the same methods, but considering just the most important features combined in different ways.

In addition, has been performed a principal component analysis to consider the possible differences on the variance of the datasets.

3 Results

In this chapter are presented the results obtained from the processing steps described in the methods. The outcomes are presented starting from the processing of the masks (to understand where is the focus), going through the classification performance on the different datasets and weights of the matrices. Finally, it is presented the comparison between the relevant features and the relative new classification performances for the datasets considering different group of features.

3.1 Mask Processing Output

In this section are presented the final masks orientation over the diffusion data images. To understand the steps done by each mask it is shown the original mask image not fitting (figure 1), the re-oriented mask image after *fslorient* application and the manual registration output (figure 2). To get the precision of the whole process, a representation of how the masks should fit with the diffusion images not correctly oriented is showed too (figure 3). Due to the fact that is possible just to visualize 2D images and the data are 3D, not every direction is shown. It has been chosen the coronal space of the brain and the auditory cortex mask, trying to show more or less the same level of depth to make a comparison.

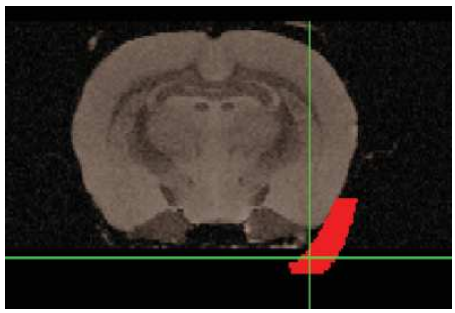

Figure 1: Image representing coronal plane of the brain and the auditory cortex mask region of interest not fitting

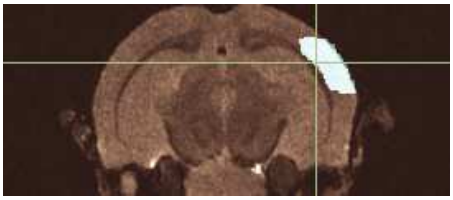

Figure 2: Image representing the coronal plane of the brain and the auditory cortex mask region of interest after the manual registration

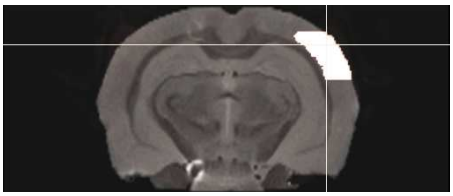

Figure 3: Image representing how the auditory cortex mask region of interest and the image should fit

3.2 Filtering Effects on Metrics

The following paragraphs present the differences of the connectograms generated before applying the SIFT filter and after. The attention is focused on the values on of the connectivity matrices and the metrics extracted. These comparison are presented for the raw data (weight based just on the counting of the streamlines between the brain regions) and weighted data (FA, MD and RD).

As mentioned, the difference of connectograms is expressed in form of *betweenness centrality*, *eigenvector centrality*, *node strength* and *global efficiency*. For the first one is applicable considering the weights on each nodes, therefore, it is different for each different matrix weight. The second metric is applied was to the network and not for every single weight. The third metric was analyzed for both matrix types (weighted and not weighted). For these three metrics the comparison is based on the difference between their values for the two classes CTRL and OBST for each one of the 10 nodes. To graphic them it has been

used a series of boxplots, is possible to visualize the mean, as a line in the boxes, and the different quartiles, as the boxes and axes. The *global efficiency* output is a single value for each subject, therefore, the comparison between the unfiltered and filtered data has been visualized in a single figure with two different lines representing the values for each subject.

The individual *betweenness centrality* for each weight and for unfiltered and filtered matrices is represented in figures 4, 5, 6 and 7. For the raw matrices is possible to see some small differences, before and after applying the filter, on the sizes of the boxplots (figure 4). In term of mean, the value for the CTRL class passes from 0.176 (unfiltered) to 0.193 (filtered). Meanwhile, for the OBST class the mean passes from 0.202 (unfiltered) to 0.180 (filtered).

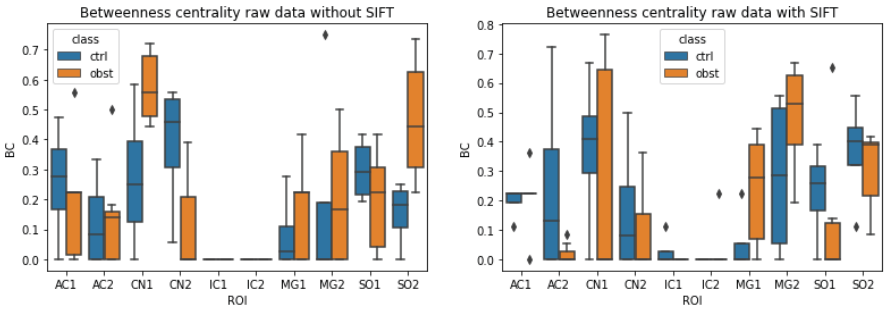

Figure 4: *Betweenness centrality* for each node between the two classes CTRL and OBST for the unfiltered raw matrix (left) and the filtered raw matrix (right)

Analyzing the output graphs of FA weighted connectograms the differences caused by SIFT filtering becomes detectable (5). In fact, is possible to note how some boxplots that are not present for the unfiltered data, appear after filtering. The means for the classes changed passing from 0.008 (unfiltered) to 0.019 (filtered) for CTRL class, and from 0.006 (unfiltered) to 0.017 (filtered) for OBST class.

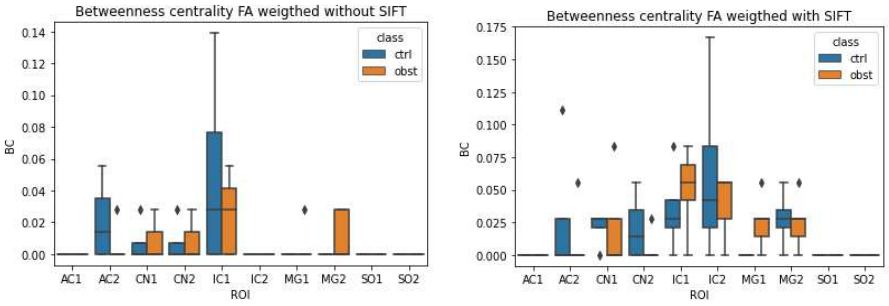

Figure 5: *Betweenness centrality* for each node between the two classes CTRL and OBST for the unfiltered FA weighted matrix (left) and the filtered FA weighted matrix (right)

For the MD weighted matrices the difference noted in the FA is more evident looking at the boxplots (figure 6). In fact, for 5 nodes, that has zero value for the unfiltered data, the *betweeness centraly* distribution value after filtering present difference between the two classes. The mean for the CTRL class passes from 0.006 (unfiltered) to 0.019 (filtered), for the OBST class it passes from 0.006 (unfiltered) to 0.017 (filtered).

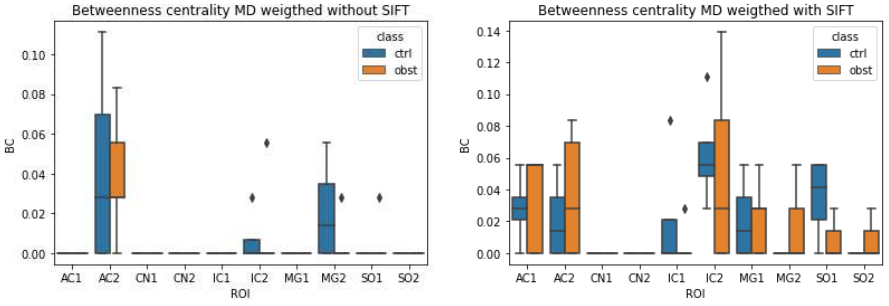

Figure 6: *Betweenness centrality* for each node between the two classes CTRL and OBST for the unfiltered MD weighted matrix (left) and the filtered MD weighted matrix (right)

The analysis on the RD weighted connectograms follows the same trend of the other weights. In fact, for 4 nodes the *betweenness centrality* passes from

zero to have positive value for at least one of the two classes. The mean values 0.007 (CTRL) and 0.006 (OBST) for the unfiltered data, 0.019 (CTRL) and 0.017 (OBST) for the filtered data.

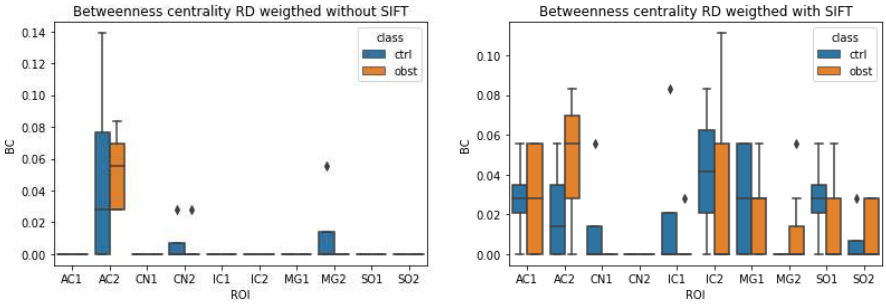

Figure 7: *Betweenness centrality* for each node between the two classes CTRL and OBST for the unfiltered RD weighted matrix (left) and the filtered RD weighted matrix (right)

The output of the *node strength* analysis is shown in figures 8, 9, 10 and 11. Analyzing visually the results for not-weighted data is possible to say that the ranges for the various nodes change after applying the filter but not drastically. In term of mean, it passes from 10.5 (unfiltered) to 9.65 (filtered) for class CTRL, and from 10.6 (unfiltered) to 9.77 (filtered) for class OBST (figure 8).

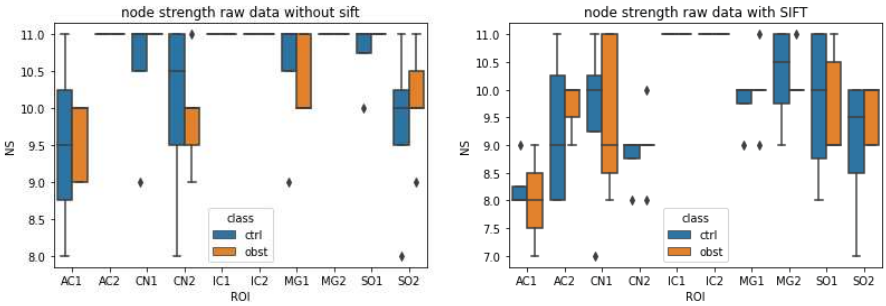

Figure 8: *Node strength* for each node between the two classes CTRL and OBST for the unfiltered data (left) and the filtered data (right)

Considering the FA weighted data, the results on the influence of filtering are visually similar to the non-weighted data (not great changes) as shown in figure 9. Evaluating the mean, for class CTRL it passes from 3.74 (unfiltered) to 3.20 (filtered), and for class OBST from 4.37 (unfiltered) to 3.75 (filtered).

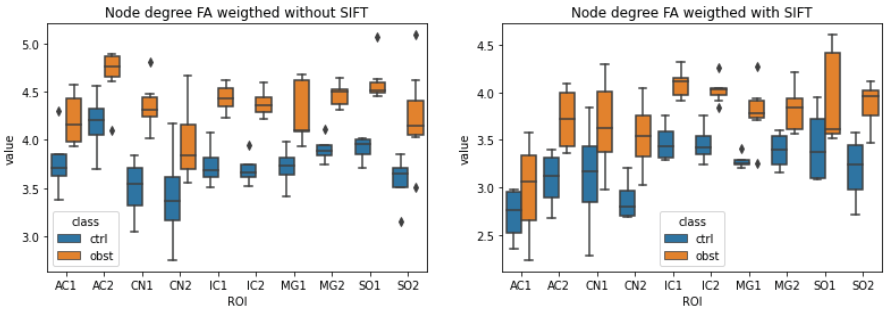

Figure 9: *Node strength* for each node between the two classes CTRL and OBST for the unfiltered FA weighted matrix (left) and the filtered FA weighted matrix (right)

Analyzing the *node strength* of the MD weighted connectograms (figure 10) is possible to notice a change on the ranges of the boxplots, wider after the SIFT application. The mean for the unfiltered data is 0.00432 (CTRL) and 0.00421 (OBST), meanwhile, for the filtered data is 0.00406 (CTRL) and 0.00397 (OBST).

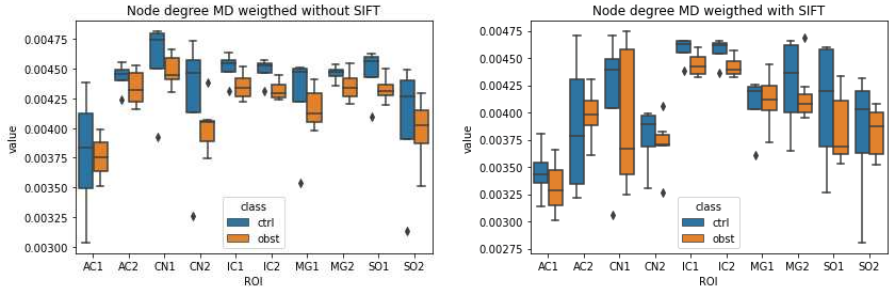

Figure 10: *Node strength* for each node between the two classes CTRL and OBST for the unfiltered MD weighted matrix (left) and the filtered MD weighted matrix (right)

The *node strength* of the RD weighted data (figure 11) showed a difference in term of ranges for the boxplots as the MD weighted data. Considering the mean, it passes from 0.00349 (unfiltered) to 0.00334 (filtered) for CTRL class, and from 0.00326 (unfiltered) to 0.00315 (filtered) for OBST class.

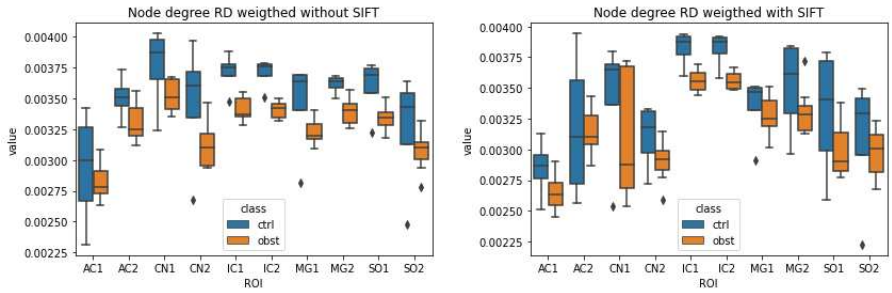

Figure 11: *Node strength* for each node between the two classes CTRL and OBST for the unfiltered RD weighted matrix (left) and the filtered RD weighted matrix (right)

The outcome of the *eigenvector centrality* is presented in figure 12. The difference between the filtered and unfiltered data is not marked, however, it is possible to note how the distribution of the value never grows, it stays in the same range or smaller (keep attention on the different y-axis unit). The mean

is 0.315 (CTRL) and 0.316 (OBST) for the unfiltered data, and 0.314 (CTRL) and 0.314 (OBST) for the filtered data.

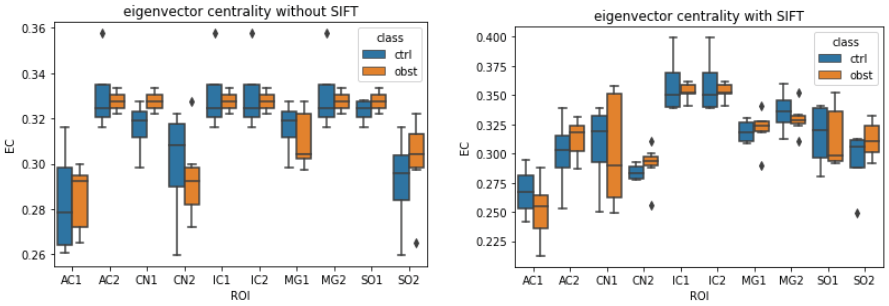

Figure 12: *Eigenvector centrality* for each node between the two classes CTRL and OBST for the unfiltered data (left) and the filtered data (right)

Global efficiency outputs are shown in figure 13 for each one of the eleven rats. The difference between the unfiltered and the filtered data is visually clear, in fact, before the SIFT application, the *global efficiency* is visually bigger than after the filter. The mean for the unfiltered data is 0.976, meanwhile, after filtering, is 0.929.

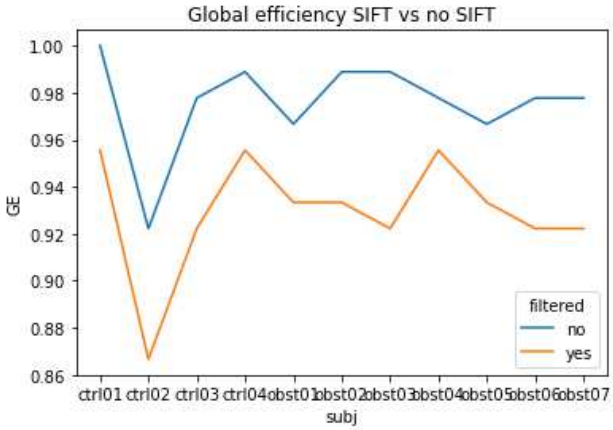

Figure 13: *Global efficiency* for each subject between the two classes CTRL and OBST for the unfiltered data and the filtered data

3.3 Classification Performance

The classification performances were evaluated with two different models, random forest and Naive-Bayes. Afterwards, as mentioned in 2.5.1, it has been given as output the datasets created from the connectivity matrices. The first experiment deals with the raw matrices, the second has been run with weighted matrices. Every run the goal is to compare the performances with unfiltered and filtered data considering the accuracy and the Kappa statistic (2.5.2), based on the factorial feature called *class* with CTRL as 1 and OBST as 2. For every experiment it has been used a cross validation leave one out to evaluate the classification performance. Moreover, it is reported the best extra parameter (*mtry* and kernel).

3.3.1 Raw Matrices

The results in table 2 show that the accuracy has been improved after the SIFT application for both the models used. furthermore, the Kappa show a big difference in the reliability of the results, in fact, for the unfiltered data is not even bigger than 0. The accuracy for the filtered data is the same for both the models, but the Kappa for Naive-Bayes is higher.

For Random Forest the best output had a *mtry* of 2 unfiltered data and 28 for filtered data. Naive-Bayes best model had *true* kernel parameter for both datasets.

Table 2: Classifier performances in percent of Random Forest and Naive-Bayes models for raw data dataset before SIFT and after SIFT

	Random Forest		**Naive-Bayes**	
	Accuracy	Kappa	Accuracy	Kappa
RAW	63.63	0	45.45	-0.18
RAW SIFT	72.72	0.29	72.72	0.38

3.3.2 Weighted Metrics

Classification performances applied to weighted datasets (FA, MD and RD) are shown in table 3. The results, in term of accuracy and Kappa, are very high. In fact, for FA weights, the models are able to distinguish the two classes perfectly with perfect Kappa value both before and after SIFT application. The unique improvement registered regards Naive-Bayes performances for MD weighted data, where the accuracy grows 0.9%. Considering the remaining outcomes, it has not been recorder any improvement, neither for accuracy nor for the Kappa.

For FA data the *mtry*s and the kernels for the best performance were the same for unfiltered and filtered data: 28 features for the Random Forest splits and *true* as kernel for Naive-Bayes.

MD weighted matrices *mtry*s were 2 for both datasets, meanwhile, kernels were different, *false* for unfiltered data and *true* for filtered data.

Regarding RD data, the extra parameters were the same for the datasets: 2 *mtry* and *true* kernel.

Table 3: Classifier performances in percent of Random Forest and Naive-Bayes models for FA, MD and RD data datasets before SIFT and after SIFT

	Random Forest		**Naive-Bayes**	
	Accuracy	Kappa	Accuracy	Kappa
FA	100	1	100	1
FA SIFT	100	1	100	1
MD	90.90	0.79	90.00	0.74
MD SIFT	90.90	0.79	90.90	0.79
RD	90.90	0.79	90.90	0.79
RD SIFT	90.90	0.79	90.90	0.79

3.4 Feature Analysis Outcome

The feature analysis has been evaluated to extract the most important features used to classify the different datasets. It has been used a Random Forest based algorithm (2.5.3) to classify the features as important or not. From the outcome of this algorithm has been created a scheme to represent the network and the different most important connections to evaluate the differences between the unfiltered and filtered data.

3.4.1 Raw matrices

Looking at figure 14 is possible to see which connections (or features) have been classified as important for the classification models. The difference between the unfiltered data and the filtered data in evident, in fact, just one connection is shared by the two (CN1-IC1). Moreover, the filtered data show more connections than the unfiltered, a total of 7 important connection (2 non plausible) against 3 (2 non plausible).

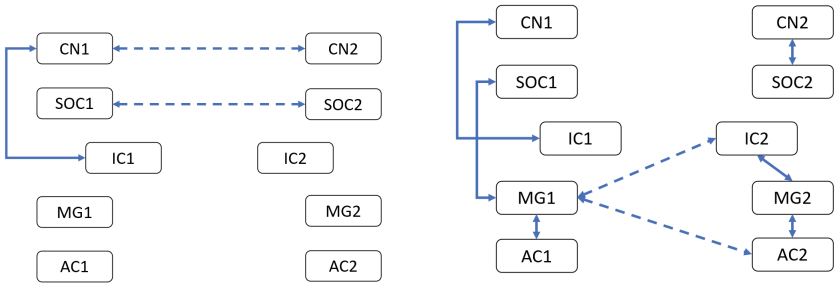

Figure 14: Graphic representation of the network and its strong connections for unfiltered RAW data (left) and filtered RAW data (right). Continuous arrows represent connections that make anatomic sense, orange boxes self connections and dashed arrows connections that not make anatomic sense

3.4.2 Weighted matrices

Considering weighted matrices the outcomes of important features analysis show differences between data before and after filtering.

As shown in figure 15, unfiltered FA weighted data has a total of 28 important connections: 22 connections between different nodes (8 non sense) and 6 self connections. Meanwhile, filtered data has a total of 26 relevant connections: 16 between different nodes (5 non sense) and 10 self connections. Many of these connections are in common. It is important to note how the non sense connections are in a small number for data after SIFT.

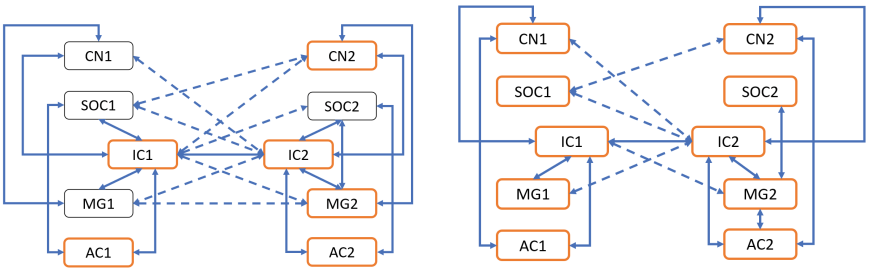

Figure 15: Graphic representation of the network and its strong connections for unfiltered FA weighted data (left) and filtered FA weighted data (right). Continuous arrows represent connections that make anatomic sense, orange boxes self connections and dashed arrows connections that not make anatomic sense

Considering MD data connections (figure 16), the differences noted in the previous graphs is kept. In fact, for unfiltered data there are 3 relevant connections plus 3 self connections, for filtered data there are 4 important connections (1 non sense) plus 3 self connections. Between the two networks there are 1 connection (CN1-SOC1) and 2 self connections (SOC1 and IC1) in common.

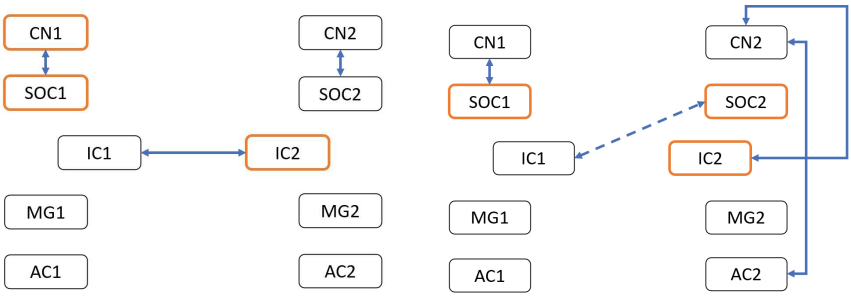

Figure 16: Graphic representation of the network and its strong connections for unfiltered MD weighted data (left) and filtered MD weighted data (right). Continuous arrows represent connections that make anatomic sense, orange boxes self connections and dashed arrows connections that not make anatomic sense

RD weighted data showed the biggest difference in the important connections analysis (figure 17). The number of non sense connections is greatly decreased after filtering and the graph looks less chaotic. For data before filtering there are 13 (5 non sense) and 3 self connections. Instead, for filtered data, the are 9 (2 non sense) and 5 self connections.

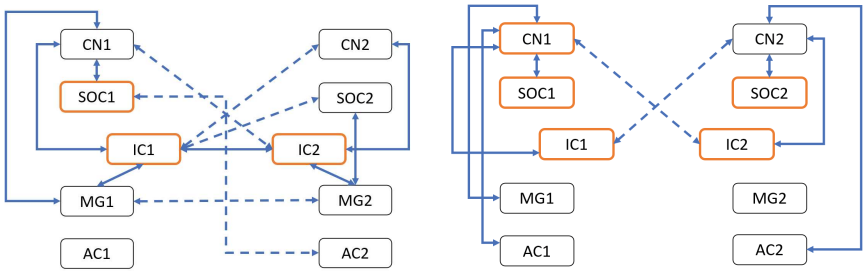

Figure 17: Graphic representation of the network and its strong connections for unfiltered RD weighted data (left) and filtered RD weighted data (right). Continuous arrows represent connections that make anatomic sense, orange boxes self connections and dashed arrows connections that not make anatomic sense

3.5 Classification Performances on Relevant Features

After the analysis for important datasets features it has been evaluated another classification with the same models and modalities of before (3.3), considering just the subset of relevant connections as features. The experiment is set in 2 steps: first one is to perform classification for raw datasets with the union and the intersection between the relevant connections, second one is to use weighted matrices as input but with the union and intersection of important features for the same weight. For this experiment it has been considered just the connections that make sense shown in the previous section.

3.5.1 RAW Matrices

Raw matrices shown better results for classification considering the union of relevant features (table 4) both for Random Forest and Naive-Bayes. In particular, for unfiltered data, the classifiers are not able to reach accuracy higher than 72.72%, meanwhile, for filtered data it is able to reach more than 90%.

Table 4: Classifier performances in percent of Random Forest and Naive-Bayes models for raw data dataset before SIFT and after SIFT considering the union of the relevant connections

	Random Forest		**Naive-Bayes**	
	Accuracy	Kappa	Accuracy	Kappa
RAW	72.72	0.30	63.63	0.21
RAW SIFT	90.90	0.79	90.90	0.79

Considering the intersection of the relevant features the improvements with filtered dataset are smaller. In fact, for Random Forest, the accuracy is the same, but with a higher Kappa. However with Naive-Bayes the performances are better.

Table 5: Classifier performances in percent of Random Forest and Naive-Bayes models for raw data dataset before SIFT and after SIFT considering the intersection of the relevant connections

	Random Forest		**Naive-Bayes**	
	Accuracy	Kappa	Accuracy	Kappa
RAW	72.72	0.30	72.72	0.30
RAW SIFT	72.72	0.37	81.81	0.56

3.5.2 Weighted Matrices

Analyzing the results from the weighted matrices as input, the performances are similar both before and after applying SIFT. In particular, considering the union of the features (table 6), for FA weighted data the values of accuracy and Kappa are the same. Meanwhile, considering MD weights, the performances are increased for both models getting a perfect classification of 100%. RD weights reached the same results for Random Forest, but, for Naive-Bayes, accuracy and Kappa are increased to 100% and 1 respectively.

Table 6: Classifier performances in percent of Random Forest and Naive-Bayes models for FA, MD and RD data datasets before SIFT and after SIFT considering the union of the relevant connections

	Random Forest		**Naive-Bayes**	
	Accuracy	Kappa	Accuracy	Kappa
FA	100	1	100	1
FA SIFT	100	1	100	1
MD	90.90	0.79	90.90	0.79
MD SIFT	100	1	100	1
RD	90.90	0.79	90.90	0.79
RD SIFT	90.90	0.79	100	1

The results considering the intersection of relevant features (table 7) are almost the same of union. FA and RD weighted data reached the same accuracy and Kappa models. Meanwhile, Random Forest with MD data increased reaching 100% both for unfiltered and filtered data, Naive-Bayes kept the same performances of the union.

Table 7: Classifier performances in percent of Random Forest and Naive-Bayes models for FA, MD and RD data datasets before SIFT and after SIFT considering the union of the relevant connections

	Random Forest		**Naive-Bayes**	
	Accuracy	Kappa	Accuracy	Kappa
FA	100	1	100	1
FA SIFT	100	1	100	1
MD	100	1	90.90	0.79
MD SIFT	100	1	100	1
RD	90.90	0.79	90.90	0.79
RD SIFT	90.90	0.79	100	1

4 Discussion

This section tries to discuss about results and gives a possible meaning about them. Possible errors made and possible future works are mentioned too.

4.1 Connectivity Metrics

The evaluated metrics are *betweenness centrality*, *node strength*, *eigenvector centrality* and *global efficiency*. Considering these graph metrics is possible to say that SIFT filtering is able to modify the weight of nodes and edges. This is supported by the fact the results in most cases are different between the unfiltered and filtered data (weighted and not). Considering the *betweenness centrality*, there is the biggest change, in fact, just looking at the boxplot graphs in section 3.2 is possible to notice how a lot of nodes, that did not have any value for unfilttered data, assumes a range of value after filtering. Interesting to note how many of the range values become smaller with SIFT, maybe it could make the outcome more accurate.

Eigenvector centrality shows similar behave as the *betweenness centrality*. Dealing with the *node strength* the results show a general increase (form unfiltered to filtered data) of the ranges of the boxplots both for the non weighted and weighted data, and both for CTRL and OBST class. These changes could mean that some weights of the connections changed with the filter. In term of mean, it does not show a big difference after the SIFT application. Meanwhile, the *global efficiency* for each subject decrease with filtering, this could be caused by the fact that many of the tracts are deleted so the connection between the various nodes counts less possible path to communicate.

4.2 Relevant Feature Analysis

Relevant features extracted with *Boruta* algorithm for the unfiltered and filtered data have a clear characteristic: important connections for unfiltered data are mostly changed after filtering with other connections, both for raw and weighted

data. Some of the features are in common though. However, it is very important to notice how the filtered data show much less nonsense connections, this could be by the fact that SIFT is able to delete them and keep the real ones.

4.3 Classification

The classification between the two classes, *ctrl* and *obst*, have had better accuracy and Kappa most of the time after filtering. Moreover, using the unfiltered dataset, the classification methods have been able just to reach the same results as with the filtered dataset. The biggest differences in performances were using the raw data, both considering all the features of the datasets both after important features selection. In fact, the increase due to the filter application with all the features, and even with the union of the important features, was $\sim$27%, from features intersection was $\sim$10%. For the whole datasets the best performances have been reached by the FA weighted, the accuracy is 100% both for Random Forest and Naive-bayes, before and after applying filter. Meanwhile, considering the reduced number of feature after selection and their union, besides FA datasets, MD weighted data reach 100% of accuracy after filtering for both classification model, as RD weighted data with Naive-Bayes after SIFT. These weighted datasets reached the best same results with the intersection of features too, the only difference was for MD unfiltered data that reached 100% accuracy with Random Forest. The improvement of performances after feature selection was expected, in fact a lot of noisy feature have been deleted.

The high performances on the weighted data could be caused by the low number of subject and, after the weighing step, it became very easy to distinguish the two classes. However, it is important to note that the rats were supposed to be easily distinguishable, as the results suggest. It would be interesting to evaluate the performances with same models but with a lot more subjects.

Raw data are the best case to show the relevance of SIFT filtering, I wonder if it would get the same improvement with a bigger dataset.

4.4 Possible Errors and Limitations

The main possible errors and limitations could have been the masks processing step. In fact, all the mask were created manually by a surgeon, the chances that the ROIs were not perfect is very high. Moreover, these masks needed to be registered from the original space position to make them fit as best as possible in the correct place. Obviously, this registration step could not have been done perfectly due to the fact manual registration was needed (2.2). These steps played a crucial role in the evaluation of tractograms and connectivity matrices.

It is important to consider the small dataset used, it was formed by 11 rats. It is relevant to take in account this detail, results from a small dataset could represent a singularity.

Tractograms generation needed a lot of parameters to be set, considering that this work deals with rats data, it was not easy to choose a correct set of parameter.

4.5 Future works

After the conclusion of this work it would be interesting to verify the good result after SIFT filtering with a bigger dataset and less specific. Introduction in the pipeline of masks generated by a default atlas would be relevant too.

5 Conclusion

In this thesis it has been studied the effect of SIFT filtering on tractograms through analysis of connectivity metrics and the classification performances of the connectivity matrices (between *ctrl* and *obst* classes) generated focusing on specifics region of the rat brain, the hearing cortex. Classification was performed with Random Forest and Naive-Bayes considering a leave one out cross-validation.

The effect of SIFT filtering is translated on a change of edge weights and nodes connectivity. These results are shown by the difference of the metrics value (*betweenness centrality*, *node strength eigenvector centrality* and *global efficiency*) before and after filtering.

Classification performances, measured with accuracy and Kappa statistic, based on the the connectivity matrices, before, and on a specific set of relevant features, after, showed improvement with filtering, or at least the same result, both for raw and weighted data. The biggest difference was achieved considering raw data (27.27% more accurate for filtered dataset). The best absolute performance was achieved with weighted dataset (FA, MD and RD) with 100% accuracy, in some cases both for unfiltered and filtered data.

Feature analysis showed an interesting outcome about the network structure. In fact, filtered data relevant connections had a smaller number of nonsense connections than unfiltered data relevant connections. The specific connections were different too, showing a different distribution of the important tracts in the network.

The results evaluated in this work bring to a conclusion: tractogram filtering is a very powerful technique that can improve the traditional tractogram generation. The improvement on classification performances supports this theory. However, due to the several number of steps needed to apply filtering, is important to weight carefully every decision on this technique.

6 State Of the Art

The following section wants to give the reader the possibility to better understand the arguments dealt with during this thesis.

6.1 - Diffusion Magnetic Resonance Imaging

Magnetic Resonance Imaging (MRI) is a non-invasive imaging technique to probe the structural environment of brain tissues applying strong magnetic fields and gradients in different directions. It makes use of the intrinsic spin of atom nuclei and its changes [1]. However, when the main objective of MRI studies involves even small tissue elements like neuron fibers of white matter, traditional MRI methods are not sufficient. It is necessary to use diffusion MRI techniques to analyze the movement of molecules inside brain tissues and their interaction with external environment. Water molecules are the most analyzed for these studies. This technique is characterized by a specific MRI sequence in the direction of the gradients and their frequency [2]. Therefore, the aim of diffusion MRI is to detect hindrances in free movement of water molecules diffusion. Basically, it is possible to recognize two different kinds of movement: isotropic (same diffusion intensity in all directions) and anisotropic (diffusion intensity dependent from direction). The parameter that regulates the desired amount of water diffusion is called b-value (s/mm2), and it represents the strongness of diffusion [3].

The main idea is to acquire different images using different direction for gradient q. However, it is too time consuming to acquire all possible signals from every direction, therefore, different techniques have been developed to evaluate diffusion characteristics with few directions in every voxel. The first one is diffusion weighted imaging (DWI) that requires just 4 directions for a single measurement of diffusion, this technique is used to characterize isotropic tissues. If the tissues are anisotropic, it could be used the diffusion tensor imaging (DTI) for analyze the main direction voxel by voxel using a tensor, and just acquiring 7 different directions [3,4]. However, these two techniques

are not useful for modern issues, where the main goal is to extract information even where there are crossing fibers. For this reason, a more advanced model has been proposed for high angular resolution diffusion imaging (HARDI) that permits to evaluate the orientation distribution functions (ODF). By analyzing the peaks of the ODF it is possible to estimate different fibers in the same voxel [4].

Diffusion MRI techniques are the base to investigate brain tissues. It is possible to characterize different tissues (DWI), analyze anisotropy and main direction (DTI), and to evaluate tractography (HARDI).

6.2.1 - Tractography

Tractography is a method used to identify and measure the pathways of fiber population for the white matter. It is the only method available to extract this information in vivo non-invasively [5,7].

It is possible to evaluate all the information about white matter structure from diffusion MRI signal, in fact, we need to analyze the distribution function of water molecules to obtain the principal directions to visualize the directional information of the axonal fiber. Furthermore, we can draw maps with each voxel represented as a vector of the tensor or, in alternative, with an ellipsoid built by the three principal directions. This relation between the diffusion tensor and the direction of the fibers is because water molecules tend to be hindered by the partition of axons. This makes the dominant direction of the diffusion even the possible axon fiber direction we are trying to detect. So, it is possible to extract the main eigen vectors of the diffusion tensor related to the principal eigen values, for each voxel, to understand how the fibers are structured [5].

The first family of methods is called deterministic tractography and assumes of the equality between the voxel-wise principal diffusion eigenvector and the line tangent to the axonal fiber belonging to the same voxel. The fiber is represented as a line called streamline, which is the discussed tangent line. It is necessary to set an initial value, as the starting point of the streamline (it is often called

as starting seed), where reconstruction is starting. This technique has stopping criteria based on local fiber orientation probability or curvature: the first is based on the value of fractional anisotropy (FA), when it falls below a certain threshold you might face with high uncertainty about diffusion direction. The second imposes a maximum curvature for the streamline, so the angle between two consecutive voxels cannot exceed a certain value [6,7].

However, there are many problems with deterministic tractography that are fundamentally ill-posed: this means this technique could lead to inaccurate results, and so to inappropriate connectivity maps empty of false positives and omit true positives. The main reasons are some limitations in using just the principal eigenvalue as the indicator for the fiber direction. In fact, the noise of the diffusion image partial volume effect could influence affect the direction of the principal eigenvector [5]. This is very important considering the possible paths of the fibers that could lead to cases where it is very difficult to estimate the correct structure. Considering conditions where there are more fibers crossing, bending, fanning, or kissing, it is not possible just to use the single diffusion direction voxel by voxel, because they can all give rise to the same MRI measurement, making it impossible to distinguish between different cases [6,7,8].

To try to overcome these problems, another type of algorithms has been developed, called Probabilistic tractography. Basically, this method, generates multiple distributions of directions from different initial points. The aspect that makes these algorithms different from deterministic ones, is that the direction of diffusion for every voxel is picked randomly based on the fiber distribution. Once the various streamlines are evaluated, probabilistic tractography take in account the tracts with the highest density [6].

Another family of methods is called Global tractography. It tries to reconstruct full track of the brain at once by finding the configuration that best describes diffusion MRI data. However, these methods, even if promising, not always permits to reach a truth solution for tractography [6].

To resolve many of the problems discussed for the previous tractography

methods it could be used a process analysis for microscopic diffusion. An example of another method proposed is q-ball imaging (QBI), based on high angular resolution diffusion imaging (HARDI). However, this method allows only a computation of the diffusion orientation distribution function (dODF) which is a blurred version of the underlying fiber distribution (fODF) and this method is very time consuming [9].

6.2.2 - Spherical Deconvolution

In tractography, the fiber tracking algorithm tries to follow the estimated fiber orientation cited yet (fODF), so it would be more useful to directly calculate it (not passing through the dODF), it allows more powerful constraints to be used. It would be more advantageous to use a free-model technique, so to have less restrictions for the analysis, and use a continuous representation of the ODF. Based on these considerations the natural choice for the best technique falls into spherical deconvolution [10].

There are multiple kinds of spherical deconvolution that differ on how they work and the representation of the fODF, but we are going to see the main characteristic of this technique to understand the mechanism. This method can estimate the fiber orientation without any prior assumptions on the number of fibers but directly from the diffusion-weighted MR signal. The central concept behind is that the signal registered from every voxel is just the sum of all the signals originated from the various fibers, weighted by their respective volume fraction, and rotated into their specific orientation. This is because we assume the diffusion characteristic from each fiber is identical in all apart from its orientation, even if not true, but it helps since the problem remains linear and the orientation is not affected by this assumption [10]. To evaluate mathematically this function (S) we can assume that it is generated by the convolution of an axially symmetric response function, R, that represents the typical diffusion-weighted signal profile of a single fiber, and the fiber orientation distribution function, fODF, that contains all the volume fraction information (every fiber

is represented by a Dirac delta function oriented as the fiber orientation). This leads us to the following equation:

$$S(\theta, \phi) = F(\theta, \phi) \otimes R(\theta) \tag{4}$$

In the equation S is the total signal, F is the fiber ODF, R is the response function, θ is the elevation angle in spherical coordinates, ϕ is the azimuthal angle in spherical coordinates [10, 11, 12].

If R is known a priori it is possible to estimate F with spherical deconvolution though a reduction to a simple set of matrixes multiplication. This is possible considering the matrixes coming from the spherical harmonic decomposition of F(θ, ϕ) and from the rotational harmonic decomposition of R(θ). Now it is possible to write the equation of deconvolution:

$$\underline{S}^n = R\underline{F}^n \tag{5}$$

S, R and F are the matrixes coming from the decomposition of the original components, n in the order of the decomposition [11].

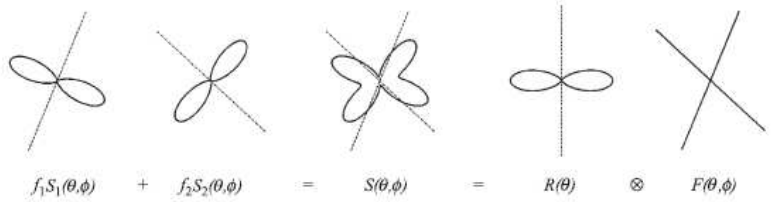

Figure 18: Possible graphical representation of spherical convolution: multiple fibers within a voxel contribute with additive signals (f_1S_1, f_2S_2) to the total signal (S). For assumption of a common fiber signal profile, fODF (F) is convoluted with fiber response function (R). Reprinted from [11] with permission of Elvesier

Despite spherical deconvolution is a very strong and useful technique, it is not perfect. In fact, it is still ill-posed and susceptible to noise (with high

b-values in particular). Moreover, the fODF and the response function need some assumptions, so it is not completely free model. In addition, spherical deconvolution approaches apply the same response function on every voxel, and this could be not true, in fact, for white matter tracts with different diameter it would be expected to influence the registered signal. Another problem that needs to be resolved is the ideal number of directions to use, in dependence of the b-values, due to the signal to noise ratio (SNR) [10, 12].

6.3.1 - Structural networks of the brain

Next step is to create the structural networks of the brain considering the measures extracted from the tractography, so it is possible to access connectivity between brain regions. To do so it is used the paths created through tractography. There are different kinds of brain networks connections achievable: with dMRI you can evaluate structural connectivity and measure the strength of it; with fMRI, usually, you can get functional and effective connectivity, where you can get even a direction of the binding between different regions [13].

Analysis of brain networks is a necessary step to reach a discrimination in connection changed due to neurodegenerative disease that could modify the neural web [14]. In literature there are many examples where structural connectivity is used to characterized and improve the knowledge of the condition [15,16,17].

Structural connectivity is based on the possibility to represent the brain composed by graphs , where every region corresponds to a node, multiple nodes can form a module (represents a bigger area of the brain), and the connections between them is called edge. The edges have not a direction and could be defined weighted; usually they are organized in a matrix called adjacency matrix (square matrix with dimension as big as the number of nodes).

However, before the analysis of connections, it is necessary to do a preprocess step where another representation of white matter is built, in addition to whole brain tractogram. This step is called parcellation of brain and consists

in defining distinct part of the brain [18]. There exist two categories of methods: cortical-parcellation-based or fiber clustering. The first one is computed, usually, from T1-weighted or T2-weighted MRI. Ones the parcellation is produced it is possible to make it collaborate with tractogram through a process of co-registration. These steps are fundamental to be able to defines all the nodes and the edges [19].

6.3.2 - Quantitative measures graph analysis for matrix

The most popular measures extracted for the connectivity matrix are computed from the modeling of dMRI signal. In particular, the characteristics of the diffusion tensor (eigenvalues and eigenvector) are used to evaluate the matrix of connection defined by the parameters considered: the principal measures are called fractional anisotropy (FA), radial diffusivities (RD), and mean diffusivities (MD). All these different weights generate different matrixes that give the possibility to do various analysis [19].

Graph measures are based on the type of analysis you want to evaluate, from local measures to global measures. At a local level, the scope is to quantify properties of a single region of interest (ROI), a node, related to its connections. It is possible to define different metrics: first is *betweenness centrality*, it consists in all the shortest paths in the network that pass through the given node. The third is participation coefficient, quantifies to what extent the node connects to different modules. The last one is the clustering coefficient, which represents the fraction of the node's neighbors that are also neighbors to each other, in other words, it is a reflex of the good or bad organization of nodes around a single node [17,18,19]. Other important metrics are *node degree* and corresponding weighted form, known as *node strength*. *Node degree* is one of the most basic metrics, it consists in the number of edges that connect a node to others. Meanwhile, *node strength* considers also the weight of each edge connected to a node [33].

Passing to the global measures, it is possible to analyze the efficiency of the structure considering the whole brain, and not only a single region or node. An

example is the *global efficiency*, which represents the capability of the transferring of information between long distances in the brain network. We consider that shortest paths mean strongest connection [17, 19, 20].

These are just some of the metrics evaluable from connectivity maps, other are described in detail in [20].

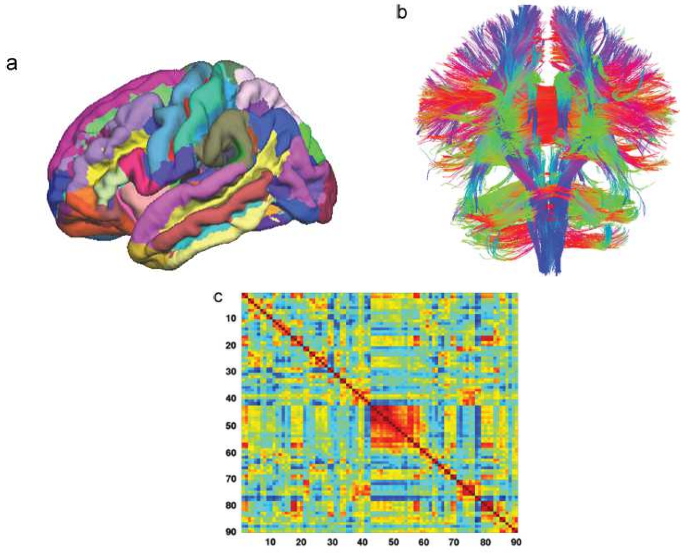

Figure 19: The figure shows, from 'a' to 'c', a human brain parcellated in different region of interest, then the output of tractography (white matter extracted) and at the end the connectivity matrix. Reprinted from [13] with the permission of Elsevier

6.4 - Tractogram filtering

As said before, one of the main problems for tractography methods is the high rate of false positives that lead to non-plausible result for streamlines. To solve this problem, many filtering techniques to apply directly to tractogram have been developed. This section will explain the principal tractogram filters.

The basic idea behind the following techniques is that dMRI signal could be generated from tractogram, so the main goal is to inspect which streamlines

can generate the original signal as close as possible and delete others. These techniques are called Linear Fascicle Evaluation (LiFE), Convex Optimization Modeling for Microstructure Informed Tractography (COMMIT) and Spherical Deconvolution Informed Filtering of Tractograms (SIFT). The first two try to minimize the distance between the raw data and the reconstructed one from the tractography, assigning weights to every streamline. So filtering is performed by discarding the streamlines with low weights [21].

SIFT differs from the other two techniques because instead of aiming for the dMRI original signal, it tries to reconstruct the fiber orientation distribution function (fODF) in every voxel. The advantage of this methods is that it adds the possibility for a biological interpretation of the process by analyzing the fODF. The filtering process for every voxel works similarly to the previous methods: the streamlines considered useless and redundant in generating the original fODF would be deleted. Important aspect to know is that SIFT does not generate weights for streamlines. The SIFT2 is the developed method of SIFT: it differs from the previous because instead of removing streamlines for each voxel, it computes weights that are then considered [21, 22, 23].

Other families of methods exist, and they differ from the one illustrated by the way they approach the problem. For example, it is possible to implement anatomical approach to identify section where streamlines are or are not supposed to be. Another family approach is based on the shapes of streamlines to decide if it is plausible or not. Moreover, other techniques are based on the possibility to cluster streamlines by the region they belong and analyze similarity [21].

Important to know is that the structural connectomes generated from the output tractogram of the filters will be different from the original one, and this is the main point where tractogram filtering plays: the possibility to get a structural connectivity more evident, even if I lose some information [22].

6.5.1 - Statistical analysis and classification

The goal of tractogram filtering, as said, is to improve the credibility of streamlines and so of the structural connectivity structure. However, this is real only if analyzed with a statistical point of view, it is necessary to classify the data with filter and no-filter to see if the performances are improved. To do that we'll see some real examples to understand what kind of analysis have been made usually.

The techniques used to perform classification are based on machine learning and deep learning concepts. In this case we are dealing with a binary classification where the subjects are classified as a patience or not. For example, in [24], they tried to classify subjects affected by Alzheimer's disease by using the Support Vector Machine (SVM), K-Nearest Neighbor (KNN), and Naive Bayes (NB) considering different aspect like the weights and the dimension of the adjacency matrix (number of nodes to consider). As described in [25], the popularity and the efficacy of deep learning techniques are getting more used, for disease prediction (including from brain networks), so they tried to use Convolutional Neural Networks (CNN) to predict Multiple Sclerosis. It is important to highlight the importance of considering different number of nodes. Other similar analysis could be done considering only the most relevant features of the matrix, after a statistic test (for example Fisher's test [15]). Another relevant result has been reached in [26], where the classification performances of connectomics in subjects with mild impairment have been improved by the tractogram filtering and selecting the features, considering more graph metrics and matrix weights.

Most of the analysis are made considering not only the entire structural connectomes but, usually, with few and most important features, that, in this case, correspond to nodes. We must remember that, due to the tractogram filters, lot of nodes could lose or gain importance in this analysis.

There are many metrics to evaluate the goodness of the classification like accuracy, precision, specificity, and sensitivity. All these performance factors

are derived from the values and operation between true positive, false positive, true negative and false negative.

6.5.2 - Evaluation of statistical results

Statistical analysis are all those steps of data processing with the goal of highlighting relevant information and characteristics. One of the way of use statistic, as said in the previous subparagraph, is machine learning. It use a process that lead to the identification of a mathematical model with the best performances possible [35]. However, it is important to know how the training and the evaluation of the classification methods assess the performances. The idea behind these tools is to compare the output of the models, for a specific feature, with the real data feature and to build a *confusion matrix*. With this matrix it is possible to get how many of the data have been classified rightly, for one class or the other. the basic measures of this techniques are accuracy, specificity and sensitivity. Accuracy is evaluated ads the ratio between the correct predictions and the total number of samples. Meanwhile, sensitivity is the ratio of all correctly classified true samples and the total of number of true samples, and specificity is the ratio between all the true negative over true negatives and false positives samples [34,35].

It is important to know that there is another measure that permits to have a feedback about the credibility of the statistical analysis performed: the Kappa statistic. This value range between -1 and 1, and reflects the possibility that the results achieved are repeatable. Value equals to 1 means total agreement in the results, -1 means total disagreement and 0 means random agreement [36, 37].

A relevant step of statistical analysis and performance evaluation is the way of perform them by splitting the dataset in training, test and validation test. A common way to perform this division is cross validation. This technique permits to create subsets for training, testing and validation by choosing the number of folds to divide the entire dataset, then the classification is performed for a

total of times as the number of folds (each time the training and test sets are changed). The output result is the mean of the outputs of each iteration [34].

6.6 - Rats auditory system

Animal brain models have been fundamental in development for studying the human brain. For example, lab animals (rodent, rats, and mice) brains have been studied due to their structural cerebral organization, that is enough like human one to permit generalization [27].

To realize how rats' auditory system is organized is fundamental to understand the brain connectivity. Principal anatomical parts are: Cochlear Nuclear Complex (CN), Superior Olivary Complex (SOC), Nuclei of the Lateral lemniscus (LL), Inferior Colliculus (IC), Medial Geniculate Body (MG) and Auditory Cortex (AC). CN receives the auditory stimulus through the auditory nerve, from here the signal is processed and transmitted to SOC. Now the signal propagates to LL and IC, and, finally, to the AC directly or through the MG [28,29,30].

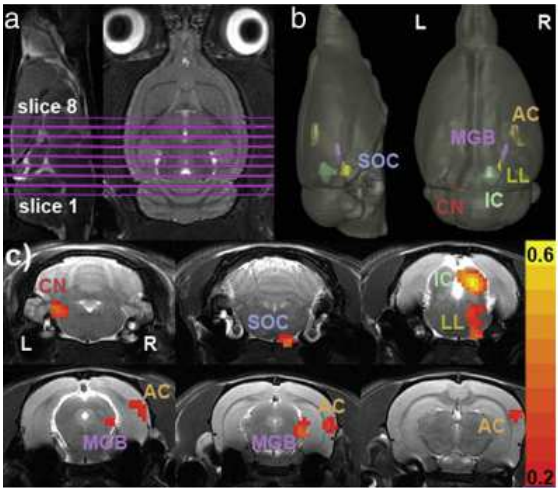

Figure 20: represented the anatomical positions of the principal section of rats' auditory system. Areas in a) are sliced in coronal slices in c). Volumes are shown in b). Yellow scale represents degree of activation when animal was exposed to sound. Reprinted from [31] with permission of Elsevier.

7 Bibliography

[1] Vijay P.B. Grover, Joshua M. Tognarelli, Mary M.E. Crossey, I. Jane Cox, Simon D. Taylor-Robinson, Mark J.W. McPhail, "Magnetic Resonance Imaging: Principles and Techniques: Lessons for Clinicians", Journal of Clinical and Experimental Hepatology, Volume 5, Issue 3, 2015, Pages 246-255, ISSN 0973-6883.

[2] Özarslan, E., & Basser, P. (2014). Introduction to Diffusion MR. Diffusion MRI: From Quantitative Measurement to In-Vivo Neuroanatomy, 3-9.

[3] Özarslan, E., & Basser, P. (2014). "Introduction to Diffusion MR. Diffusion MRI: From Quantitative Measurement to In-Vivo Neuroanatomy", 3-9.

[4] Wang, T., Shi, F., Jin, Y., Yap, P., Wee, C., Zhang, J., . . . Shen, D. (2016). Multilevel Deficiency of White Matter Connectivity Networks in Alzheimer's Disease: A Diffusion MRI Study with DTI and HARDI Models. Journal of Neural Transplantation & Plasticity, 2016, 2947136-14.

[5] Behrens, T., Sotiropoulos, S., & Jbabdi, S. (2013). MR Diffusion Tractography. In Diffusion MRI: From Quantitative Measurement to In vivo Neuroanatomy: Second Edition (pp. 429-451).

[6] Jeurissen, B., Descoteaux, M., Mori, S., & Leemans, A. (2019). Diffusion MRI fiber tractography of the brain. NMR in Biomedicine, 32(4), E3785-N/a.

[7] Rheault, F., Poulin, P., Valcourt Caron, A., St-Onge, E., & Descoteaux, M. (2020). Common misconceptions, hidden biases and modern challenges of dMRI tractography. Journal of Neural Engineering, 17(1), 011001.

[8] Jbabdi, S., & Johansen-Berg, H. (2011). Tractography: Where Do We Go from Here? Brain Connectivity, 1(3), 169-183.

[9] Aganj, I., Lenglet, C., Sapiro, G., Yacoub, E., Ugurbil, K., & Harel, N. (2010). Reconstruction of the orientation distribution function in single- and multiple-shell q-ball imaging within constant solid angle. Magnetic Resonance in Medicine, 64(2), 554-566.

[10] Dell'Acqua, F., & Tournier, J. (2019). Modelling white matter with spherical deconvolution: How and why? NMR in Biomedicine, 32(4), E3945-

N/a.

[11] Tournier, J., Calamante, F., Gadian, D., & Connelly, A. (2004). Direct estimation of the fiber orientation density function from diffusion-weighted MRI data using spherical deconvolution. NeuroImage (Orlando, Fla.), 23(3), 1176-1185.

[12] Tournier, J., Yeh, C., Calamante, F., Cho, K., Connelly, A., & Lin, C. (2008). Resolving crossing fibres using constrained spherical deconvolution: Validation using diffusion-weighted imaging phantom data. NeuroImage (Orlando, Fla.), 42(2), 617-625.

[13] Fornito, A., & Bullmore, E. (2014). Connectomics: A new paradigm for understanding brain disease. European Neuropsychopharmacology, 25(5), 733-748.

[14] Edison, P. (2020). Brain Connectivity: Structural Integrity and Brain Function. Brain Connectivity, 10(1), 1-2.

[15] Multivariate regression analysis of structural MRI connectivity matrices in alzheimer's disease

[16] Rasero, J., Amoroso, N., Rocca, M., Tangaro, S., Bellotti, R., & Stramaglia, S. (2017). Multivariate regression analysis of structural MRI connectivity matrices in Alzheimer's disease. PloS One, 12(11), E0187281.

[17] Roine, T., Roine, U., Tokola, A., Balk, M., Mannerkoski, M., Åberg, L., . . . Autti, T. (2019). Topological alterations of the structural brain connectivity network in children with juvenile neuronal ceroid lipofuscinosis. American Journal of Neuroradiology: AJNR, 40(12), 2146-2153.

[18] Eickhoff, S., Yeo, B., & Genon, S. (2018). Imaging-based parcellations of the human brain. Nature Reviews. Neuroscience, 19(11), 672-686.

[19] Zhang, F., Daducci, A., He, Y., Schiavi, S., Seguin, C., Smith, R., . . . O'Donnell, L. (2022). Quantitative mapping of the brain's structural connectivity using diffusion MRI tractography: A review. NeuroImage (Orlando, Fla.), 249, 118870.

[20] Rubinov, M., & Sporns, O. (2010). Complex network measures of brain connectivity: Uses and interpretations. NeuroImage (Orlando, Fla.), 52(3),

1059-1069.

[21] Jörgens, D., Descoteaux, M., & Moreno, R. (2021). Challenges for Tractogram Filtering. In Mathematics and Visualization (Mathematics and Visualization, pp. 149-168).

[22] Frigo, M., Deslauriers-Gauthier, S., Parker, D., Ismail, A., Kim, J., Verma, R., & Deriche, R. (2020). Diffusion MRI tractography filtering techniques change the topology of structural connectomes. Journal of Neural Engineering, 17(6), Journal of neural engineering, 2020-11-11, Vol.17 (6).

[23] Hain Antonia, 2021, Assessing individual streamline plausibility through randomized Spherical-Deconvolution Informed Tractogram Filtering, KTH thesis

[24] Shao, J., Myers, N., Yang, Q., Feng, J., Plant, C., Böhm, C., . . . Sorg, C. (2012). Prediction of Alzheimer's disease using individual structural connectivity networks. Neurobiology of Aging, 33(12), 2756-2765.

[25] Marzullo, A., Kocevar, G., Stamile, C., Calimeri, F., Terracina, G., Durand-Dubief, F., & Sappey-Marinier, D. (2019). Prediction of Multiple Sclerosis Patient Disability from Structural Connectivity using Convolutional Neural Networks. 2019 41st Annual International Conference of the IEEE Engineering in Medicine and Biology Society (EMBC), 2087-2090.

[26] Kopff Marvin, 2020, Impact of tractogram filtering and graph creation for structural connectomics in subjects with mild cognitive impairment, KTH thesis

[27] Halliwell, C. (2018). The Role of Animal Models in Developmental Brain Research. In The Neurobiology of Brain and Behavioral Development (pp. 81-95).

[28] Kraft Sandra, 2016, Routine Development for Artefact Correction and Information Extraction from Diffusion Weighted Echo Planar Images of Rats, KTH thesis

[29] Savva Androula, 2019, Assessment of functional connectivity impairment in rat brains, KTH thesis

[30] Manuel S. Malmierca, Chapter 29 - Auditory System, Editor(s): George

Paxinos, The Rat Nervous System (Fourth Edition), Academic Press, 2015, Pages 865-946, ISBN 9780123742452,

[31] Cheung, M., Lau, C., Zhou, I., Chan, K., Cheng, J., Zhang, J., . . . Wu, E. (2012). BOLD fMRI investigation of the rat auditory pathway and tonotopic organization. NeuroImage (Orlando, Fla.), 60(2), 1205-1211.

[32] Tournier, J., Calamante, F., & Connelly, A. (2012). MRtrix: Diffusion tractography in crossing fiber regions. International Journal of Imaging Systems and Technology, 22(1), 53-66.

[33] Fornito, Alex, Andrew Zalesky, and Edward Bullmore. "Chapter 4 - Node Degree and Strength." Fundamentals of Brain Network Analysis. Elsevier Inc, 2016. 115–136. Web.

[34] Zhou, Zhi-Hua. Machine Learning. Gateway East, Singapore: Springer, 2021. Print.

[35] Jeyaraman, Brindha Priyadarshini, Ludvig Renbo Olsen, and Monicah Wambugu. Practical Machine Learning with R: Define, Build, and Evaluate Machine Learning Models for Real-World Applications. Birmingham: Packt Publishing, Limited, 2019. Print.

[36] García-Álvarez, David. et al. Land Use Cover Datasets and Validation Tools: Validation Practices with QGIS. Cham: Springer International Publishing AG, 2022. Print.

[37] Allouche, Omri, Asaf Tsoar, and Ronen Kadmon. "Assessing the Accuracy of Species Distribution Models: Prevalence, Kappa and the True Skill Statistic (TSS)." The Journal of applied ecology 43.6 (2006): 1223–1232. Web.

[38] Im, Sang-Jin et al. "Deterministic Tractography Analysis of Rat Brain Using SIGMA Atlas in 9.4T MRI." Brain sciences 11.12 (2021): 1656–. Web.